Journal of Nuclear Materials 313–316 (2003) 664–669

journal of nuclear materials

www.elsevier.com/locate/jnucmat

Comprehensive modeling of ELMs and their effect on plasma-facing surfaces during normal tokamak operation ☆

A. Hassanein *, I. Konkashbaev

Argonne National Laboratory, 9700 S. Cass Avenue Building, 308, Argonne, IL 60439, USA

Abstract

During the normal operation of the high confinement regime (H-mode) in next generation tokamaks, edge-localized modes (ELMs) are a serious concern for divertor plasma-facing components. The periodic relaxation of edge pressure gradient results in pulses of energy and particles transported across the Separatrix to the scrape-off-layer (SOL) and eventually to the divertor surface. ELMs could, therefore, result in cyclic thermal stresses, excessive target erosion, and consequently shorter divertor lifetime. In this study a comprehensive two-fluid model has been developed to integrate SOL parameters during ELMs with divertor surface evolution (melting, vaporization, vapor cloud dynamics, and macroscopic spallation) for different ELM parameters. Calculations were performed using the HEIGHTS numerical simulation package. Initial results indicate that high-power ELMs in ITER-like machines can cause serious damage to divertor components, may terminate plasma in disruptions, and may affect subsequent plasma operations due to extensive contamination.

Keywords: ELMs; Disruptions; Vapor shielding; Erosion; Divertor; HEIGHTS package

1. Introduction

Recently, edge-localized modes (ELMs) have been the focus of increasing attention for tokamak reactor design because of the potential impact of the high heat pulses on divertor design and lifetime in future reactors such as ITER. The importance of ELMs arises from a number of concerns such as limiting energy confinement, providing density control and limiting buildup of impurities, broadening the scrape-off-layer (SOL) density profile, causing large heat pulses on the plasma-facing components (PFCs), and increasing the sputtering of divertor materials.

During ELMs, part of the tokamak's total plasma energy, Q_{ELM} of ≈0.01–0.1 of core plasma energy, Q_{core}, is released and deposited on the divertor surface over a duration of ≈0.1–1 ms with a frequency of ≈10–20 Hz. The incoming power from the SOL to the divertor plate in ITER-like devices during an ELM can then increase from ≈5 to ≈300–3000 MW/m^2. The mass losses of divertor materials strongly depend on the power deposited. At low power deposition, the surface temperature of the PFC, such as Be and C, will not exceed the melting temperature, and mass losses due to vaporization are small. However, with ELM frequencies of 10–20 Hz, thermal cycling takes place and can result in thermal stresses and fatigue. At high Q_{ELM}, however, the resulting high surface temperature causes vapor-cloud formation with similar consequences to plasma disruption [1]. Vapor shielding decreases energy deposition at the surface but increases radiation flux to nearby components. Metallic PFCs will melt, and liquid metal flow instabilities occur, with increased mass losses due to magnetohydrodynamic effects and bubble splashing as well as and atomic vaporization [2].

The mechanisms responsible for the rapid loss of plasma from the core edge during ELMs have not been

---

☆ Presented at the Fifteenth International Conference on Plasma Surface Interaction (PSI-15) 27–31 May 2002, Gifu, Japan.

* Corresponding author. Tel.: +1-630 252 5889; fax: +1-630 252 3250.

E-mail address: hassanein@anl.gov (A. Hassanein).

0022-3115/03/$ - see front matter © 2003 Elsevier Science B.V. All rights reserved.
PII: S0022-3115(02)01376-4

clearly identified. Some of the suggested mechanisms include parallel convection along suddenly opened field lines produced by island formation, turbulent radial transport due to electrostatic or electromagnetic fluctuations, and radial convection due to large-scale-length potential structures [3,4]. Therefore, to predict consequences of ELMs such as enhanced mass losses and contamination of core plasma, a simplified model of plasma behavior during ELMs has been developed, taking into account features mainly inherent in most current fusion machines.

Duration of ELMs in ITER-like machines is expected to be $0.1 < \tau_{\rm ELM} < 1$ ms; however, the duration for most ELMs is near $\tau_{\rm ELM} \approx 1$ ms. During an ELM, a fraction of tokamak plasma energy, $Q_{\rm ELM} = \eta Q_{\rm core}$, escapes to the SOL. This energy can consist of a conduction part due to thermal conduction and a convection part carried by the diffusing particles.

In our model, it is assumed that the core plasma energy is lost to SOL within a region of radii from $R_{\rm ELM}$ to $R_{\rm S}$ (radius at Separatrix). Therefore, $Q_{\rm ELM}$ is equal to the plasma energy contained between $R_{\rm ELM}$ and $R_{\rm S}$. The available experimental data indicate that the dynamics of ELMs is stochastic as a result of large-scale (macroscopic) plasma motion. Therefore our model assumes that the energy and particles losses across magnetic field are diffusive, with some enhanced diffusion coefficient $D_\perp \approx 5$ m^2/s, which is about ten times more than the diffusion coefficient during normal operation.

2. Model of SOL during ELMs

According to our first assumption, one can find the number of particles (DT ions) that escape to the SOL during an ELM, $N_{\rm ELM}$, corresponding to an energy $Q_{\rm ELM}$:

$$Q_{\rm ELM} = \int_{R_{\rm ELM}}^{R_{\rm s}} \frac{3}{2} k(T_{\rm i} + Z_{\rm eff} T_{\rm e}) n_{\rm i}(r) 2\pi R \cdot 2\pi r \, {\rm d}r = \frac{3}{2} k T_{\rm mean}(1 + Z_{\rm eff}) N_{\rm ELM} = \eta Q_0, \qquad (1)$$

where $T_{\rm mean}$ is the average temperature of ions and electrons and $Z_{\rm eff}$ is the effective charge state in this region.

Because of the large uncertainties in ELM physics, it is more appropriate to use values that are measured directly, such as $\tau_{\rm ELM}$, than $D_\perp$ and the total energy deposited onto the divertor plate, $Q_{\rm load}$.

Fig. 1 shows the predicted ELM relative parameters as a function of radial position starting from the Separatrix ($R_{\rm S} = 2$ m) and going inward to $R_{\rm ELM}$ toward the center. For example, for $Q_{\rm ELM} \approx 1\%\ Q_0$ (i.e., $\eta = Q_{\rm ELM}/Q_0 = 0.01$), this region corresponds to a radius $R_{\rm ELM} = R_{\rm S} - \Delta R_{\rm ELM} = 2 - 0.16 = 1.84$ m, $N_{\rm ELM} \approx 0.045 N_0 = 0.2 \times 10^{22}$, and $T_{\rm mean} \approx 1.05$ keV. For $Q_{\rm ELM} \approx 10\%\ Q_0$ ($\eta = 0.10$), this corresponds to radius $R_{\rm ELM} = 1.64$ m, $N_{\rm ELM} = 0.22 N_0$, and $T_{\rm mean} \approx 2.4$ keV. The main values used are $T_0 = 10$ keV, $n_0 = 10^{20}$ m^{-3}, $Q_0 = 0.126 \times 10^9$ J, and $N_0 = 4.0 \times 10^{22}$ for an ITER-like device.

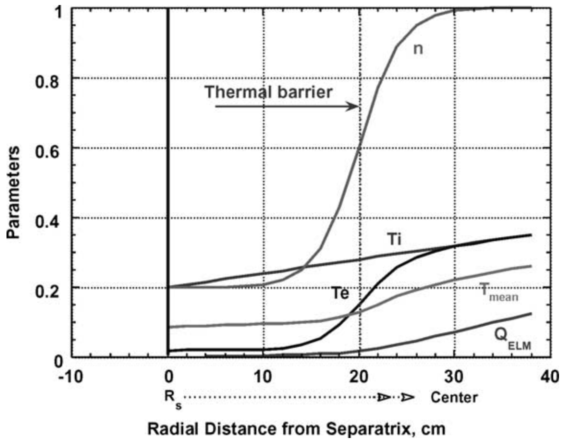

Fig. 1. Predicted ELM relative parameters as a function of radial position from Separatrix and inward to $R_{\rm ELM}$.

The large increase in both particle and heat flux is ξ times higher than the normal operation, i.e., $\xi = \eta \tau_{\rm E}/\tau_{\rm ELM} \gg 1$. This condition will result in significant increases in mass losses of the divertor plate (vaporization, sputtering, brittle destruction, and liquid splashing). To predict these losses and potential contamination of core plasma, two problems must be solved: the dynamics and structure of particles in SOL, and the interaction of particle/heat fluxes from the SOL with divertor plate materials.

During normal operation, the plasma in SOL is highly collisional, i.e., the path length, λ of ions and electrons at $T \approx 100$ eV is less than the connection length $L_{\rm con} = 2L_\parallel$ (where $L_\parallel$ is the parallel distance between the two divertor plates), i.e., $\lambda \ll 2L_\parallel$. However, during ELMs, λ ($T_{\rm mean} > 1$ keV) is much larger than the connection length, and $\lambda \gg 2L_\parallel$. Therefore, the SOL plasma during ELMs is collisionless and requires a different treatment than during normal operation.

We should emphasize that the term 'collisionless' used here does not mean that collisions can always be neglected. The term is used only to indicate that the ion and electron path length is much greater than the connection length, but electrons oscillating between plates located at distances much shorter than the particle path length (collisionless in space) will have lifetimes determined by collisions (collisional in time). Thus, the SOL during ELMs is similar to the situation of the SOL during the normal operation regime with enhanced confinement [3,4] or during a disruption [5].

One main feature of the collisionless SOL plasma is that the edge plasma acts as an electrostatic trap for electrons, since electrons which originally have parallel energy that is lower than the wall potential energy, φ, will be trapped between the inner and outer divertor plates. To obtain the potential φ and corresponding net heat flux of ions and electrons to the divertor plate, one can make use of previous models [6]. For conditions of the SOL during ELMs, the negative potential, φ, at the boundary between the SOL and the ionized vapor cloud near the divertor surface is $|e\varphi| \geqslant kT_\mathrm{e}$, where T_e is the electron temperature at the corresponding magnetic field line. Ions and electrons with energy parallel to magnetic field lines, $E_\parallel$, $e > \varphi$, leave the SOL directly (escaping particles). A simple model based on similar physical processes described in Ref. [6] is used to calculate particle fluxes from the SOL to the divertor surface.

3. Ion and electron particles and energy fluxes

The ions escaping the SOL with increased parallel energy, $E_{\parallel,\mathrm{i}}$, due to acceleration in potential φ will have increased velocity U_i and decreased density n_i:

$$E_{\parallel,\mathrm{i}} = E_{\parallel,\mathrm{i}0} - e\varphi, \quad U_\mathrm{i} = V_{\mathrm{i}0}(1 + \mathrm{e}^{\psi}),$$
$$\psi = -\frac{e\varphi}{kT_\mathrm{e}}, \quad n_\mathrm{i} = n_0/(1 + \mathrm{e}^{\psi}), \tag{2}$$

where n_0 is the ion density in a given magnetic field line. The ion particle flux and ion heat flux, W_i, leaving the SOL is the same as in the absence of potential. However, the ion heat flux, $W_{\mathrm{i}d}$, reaching the evolving vapor-cloud above the divertor surface increases due to acceleration in the z-direction due to the potential jump:

$$W_{\mathrm{i}d} = W_{\mathrm{i}0} + \Delta W_\varphi, \quad \Delta W_\varphi = \frac{3}{2}\psi W_{\mathrm{i}0},$$
$$W_{\mathrm{i}0} = \frac{3}{2}kT_{\mathrm{mean}} n_0 V_{\mathrm{i}0}. \tag{3}$$

Electrons escape the SOL with a parallel energy $E_\parallel$, $e > -e\varphi$; thus, the average velocity U_e, density $n_{\mathrm{e}d}$, total flux of escaping electrons S_e, and corresponding heat flux W_e are determined by the potential φ. The ion heat flux increases by ΔW_φ because of acceleration in the negative potential, φ, created by electrons. This means that electrons spend the same power, ΔW_φ, to maintain such negative potential. Thus, the full electron heat loss, $W_{\mathrm{e}\parallel}$, along magnetic field lines is

$$W_{\mathrm{e}\parallel} = W_\mathrm{e} + \Delta W_\varphi, \quad W_\mathrm{e} = \tfrac{3}{2}kT_\mathrm{e} n_0 V_{\mathrm{e}0}\mathrm{e}^{-\psi}, \quad n_{\mathrm{e}d} = n_0\mathrm{e}^{-\psi}. \tag{4}$$

In addition, the potential φ is determined by the assumption that fluxes of electrons and ions are equal:

$$S_{\mathrm{e}\parallel} = nV_{T_\mathrm{e}}\mathrm{e}^{-\psi} = S_{\mathrm{i}\parallel} = nV_{T_\mathrm{i}} = S_0,$$
$$\psi = -\frac{e\varphi}{kT_\mathrm{e}} = \ln\sqrt{\frac{m_\mathrm{i}T_\mathrm{e}}{m_\mathrm{e}T_\mathrm{i}}}. \tag{5}$$

Because fluxes of electrons and ions are assumed equal, the density of escaping electrons, $n_{\mathrm{e}d}$, is less than the density of ions in the SOL, $n_{\mathrm{i}d}$, where $n_{\mathrm{i}d}/n_{\mathrm{e}d} = \exp(\psi) \gg 1$.

Neutralization of ion charge is achieved not only by the escaping electrons but also by trapped electrons and cold electrons coming from the vapor cloud above the divertor surface. Therefore, electron and ion densities in SOL are equal. Cold electrons during their flight in the SOL between divertor plates can be thermalized due to binary and turbulent collision [6].

4. Energy and mass balance

In the above discussion, we assume that ions and electrons diffuse across magnetic field lines with an effective diffusion coefficient $D_\perp$. The ions freely leave the SOL, escaping electrons freely leave the SOL, and trapped electrons leave the SOL by diffusion in momentum space. Because the energy of these diffusing trapped electrons is near zero, their contribution to the heat fluxes is neglected. Therefore, the mass conservation law has the form

$$\frac{\partial n}{\partial t} = \frac{\partial S_\perp}{\partial r} - \frac{S_\parallel}{L_\parallel} = 0, \quad S_\perp = D_\perp\frac{\partial n}{\partial r}, \quad S_\parallel = nV_{\mathrm{i}0}. \tag{6}$$

The thermal energy also diffuses with the same diffusion coefficient carrying energies of ions, 3/2 kT_i, and electrons, 3/2 kT_e. Therefore, the energy conservation law has the form

$$\frac{3}{2}kn\frac{\partial T_\mathrm{i}}{\partial t} = \frac{\partial W_{\mathrm{i}\perp}}{\partial r} - \frac{W_{\mathrm{i}\parallel}}{L_\parallel} + \frac{3}{2}kn\frac{T_\mathrm{e} - T_\mathrm{i}}{\tau^\varepsilon_{\mathrm{ei}}} = 0,$$
$$\tau^\varepsilon_{\mathrm{ei}} = \frac{m_\mathrm{i}}{2m_\mathrm{e}}\tau_\mathrm{e}. \tag{7}$$

The boundary conditions at the Separatrix $(r = 0)$ and the SOL edge $(r = \infty)$ are

$$S_\perp = D_\perp\frac{\partial n}{\partial r} = \frac{1}{2\pi R}\frac{1}{2\pi a}\frac{N_{\mathrm{ELM}}}{\tau_{\mathrm{ELM}}},$$
$$W_{\mathrm{i}\perp} = W_{\mathrm{e}\perp} = \frac{3}{2}kT_{\mathrm{mean}}S_\perp, \tag{8}$$

$$S_\perp = 0, \quad W_{\mathrm{i}\perp} = W_{\mathrm{e}\perp} = 0, \tag{9}$$

where N_{ELM} is again the total number of ions leaving the edge core plasma to the SOL.

The density equation has the solution

$$n = n_0\mathrm{e}^{-(r/\lambda_\mathrm{i})}, \quad n_0 = \frac{S_{\perp 0}\lambda_\mathrm{i}}{D_\perp}, \quad \lambda_\mathrm{i} = \sqrt{\frac{D_\perp L_\parallel}{V_{\mathrm{i}0}}}. \tag{10}$$

At these conditions, the temperature of ions is constant along the radius. The energy equation for electrons is written as

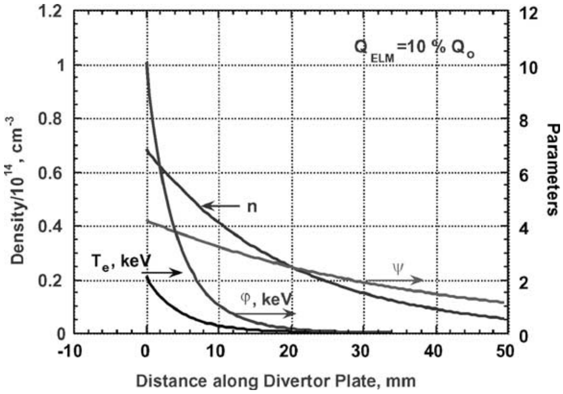

Fig. 2. Calculated ELM density n, electron temperature T_e, potential φ, and normalized potential ψ for typical tokamak parameters.

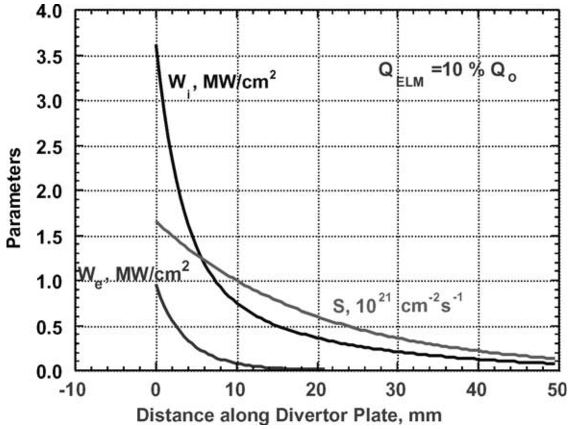

Fig. 3. Calculated spatial distribution of particle flux S, electron heat flux W_e, and ion heat flux W_i during an ELM.

$$\frac{\partial T_e}{\partial r} = -\frac{T_e}{\lambda_i} \ln\left(\sqrt{\frac{m_i T_e}{m_e T_i}}\right) \tag{11}$$

and is solved numerically. Fig. 2 shows the density n, electron temperature T_e, potential φ, and normalized potential ψ for the tokamak parameters of $R_{\text{major}} = 6$ m, a(minor radius) $= 2$ m, $L_{\text{II}} \approx 2\pi R_{\text{major}} = 37.67$ m, $T_0 = 10$ keV, $n = 10^{20}$ m^{-3}, and $D_\perp = 5$ m^2/s. Fig. 3 shows the calculated spatial distribution of particle flux S, and the electron and ion heat fluxes (W_e and W_i, respectively). These values determine the surface evolution of the divertor plate.

5. Interaction of incident particles with divertor plate

The integrated HEIGHTS package solves problems related to particle energy deposition, evolution of surface materials, debris formation, vapor radiation magnetohydrodynamics, and erosion physics. This model has been enhanced and used in this analysis. The enhancement includes development of a two-fluid hydrodynamic mixing model, where the incident DT plasma is treated separately from the eroded debris cloud of the divertor materials. Only surface vaporization is considered as the main erosion mechanism in this study. We used the forward–reverse radiation transport method for both line and continuum radiation with detail line resolution of the vapor plasma. Parametric studies were completed for different ELM durations (from 0.1 to 1 ms) and different ELM intensities (1–10% Q_0). Two potential divertor materials were analyzed in this work, lithium and carbon.

Each flux line that strikes the divertor plate was assumed to have two-dimensional components. Flux lines were distinguished by their distance from the strike point, where the tokamak Separatrix strikes the divertor plate at $r = 0$. Input parameters were chosen under the assumption that the SOL width expands 10 times its size at the divertor surface. The effective size of the SOL at the midplane was calculated to be 1.98 cm for ions and 0.47 cm for electrons.

For example, for $\eta = 0.1$, $T_{\text{mean}} = 2.4$ keV, and density of ion/electron at $r = 0$ (at Separatrix in midplane) $n_0 = 0.7 \times 10^{20}$ m^{-3}, the maximum energy density carried by ions at the midplane is 3.6, and 0.36 MW/cm^2 at the strike point. For electrons, the maximum energy density is 0.95 MW/cm^2 at the midplane and 0.095 MW/cm^2 at the strike point. The ion energy at the strike point $E_i = (1 + \psi)T_{\text{mean}} = 12.5$ keV, and the electron energy at the strike point $E_e = T_{\text{mean}} = 2.4$ keV. The flux at the strike point $S_{\text{ELM}} = n_0 V_i(T_{\text{mean}}) = 0.67 \times 10^{26}$ m^2 s^{-1}. Therefore, the ELM model is actually similar to disruption physics and analysis but with lower total deposited energy and lower incoming particle kinetic energy (about 2 keV instead of 10 keV). The density of incoming DT particles stopped in the vapor cloud above the surface is comparable or above the vapor density of the divertor surface. Therefore, the two-fluid mixing model was developed. The front part of the vapor cloud mainly consists of stopped DT particles. Other details concerning models and physics of the plasma-material interaction during a disruption are included in Ref. [7].

Fig. 4 shows the liquid Li response to an ELM with different percent of Q_0 deposited over a duration of 1 ms. The erosion from Li vaporization increases significantly with deposited energy because of the exponential increase of the vaporization rate. At higher ELM energy, more than 90% of the incident energy is absorbed by the vapor cloud, and 80% is radiated to nearby areas. Therefore, vapor shielding is also effective during ELMs. The temperature of the cloud front is high, ≈40–50 eV, because the front part of the cloud consists of DT ions. The plate surface temperature is rather high >2000 K,

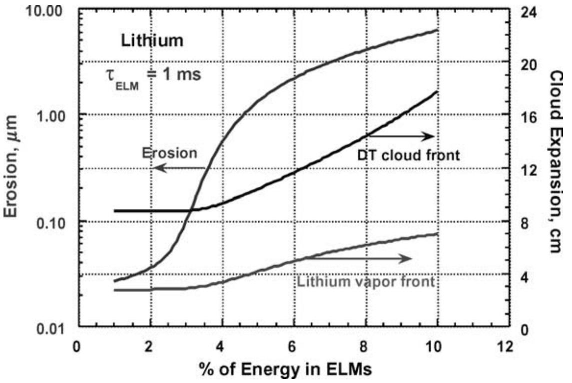

Fig. 4. Liquid Li response to an ELM with different percent of Q_0 deposited in 1 ms.

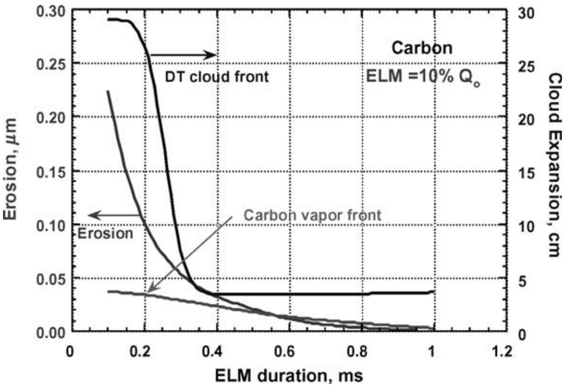

Fig. 5. Carbon plate erosion and vapor expansion as a function of ELM duration for an energy of 10% Q_0.

which results in a high erosion rate because the saturation pressure exceeds the vapor cloud pressure of a few atmospheres. Vapor expansion above the divertor surface also depends on deposited energy.

The critical factor is the net threshold power to the divertor surface, which determines the surface temperature at which the saturation pressure exceeds the cloud pressure of a few atmospheres. The cloud pressure is determined, however, by the DT flux momentum and diffusion across the magnetic field. Because the front of the cloud consists mainly of DT with high conductivity, this condition results in less diffusion and, consequently, high cloud pressure. For an ELM with $\eta = 0.1$, the erosion rate and the expansion of the vapor cloud front are high. Lithium vapor can reach the X-point that can result in contamination of the core plasma and terminate the plasma in a disruption. At ELM power below the threshold the erosion rate is tolerable, Li vapor expansion is <10 cm, and plasma contamination is low.

Because the temperature of the divertor surface can exceed the threshold for splashing during high-power ELMs, macroscopic losses in the form of liquid droplets can take place. In the case of a well-confined vapor cloud without turbulence, these droplets vaporize by radiation and shield the divertor surface; therefore, the erosion rate will not significantly increase [7]. However, if vapor turbulence exists, the erosion rate can increase substantially, and plasma contamination/termination would be a serious problem.

Fig. 5 shows the carbon plate erosion and vapor expansion as a function of ELM duration for an energy of 10% Q_0. For $\tau_{\mathrm{ELM}} < 0.3$ ms, the erosion and the DT cloud front expansion increase significantly, reaching ≈0.25 μm and $X \approx 30$ cm, respectively, at $\tau_{\mathrm{ELM}} < 0.2$ ms. For $\tau_{\mathrm{ELM}} = 1$ ms the erosion is negligible for ELM energy $\leqslant 10\%$ Q_0. In addition, most cloud volume (80%) is contained by DT, and the carbon vapor expands only to <5 cm, even for powerful ELMs (10% Q_0) with $\tau_{\mathrm{ELM}} = 0.1$ ms. This condition helps reduce core plasma contamination.

6. Summary

ELMs may be a serious concern for plasma-facing components during normal operation of the next generation tokamaks. To study this problem, a two-fluid model has been developed to integrate SOL parameters during ELMs with divertor surface evolution (melting, vaporization, vapor cloud dynamics, and macroscopic erosion). Calculations were performed using the HEIGHTS numerical simulation package. Initial results indicate an ELM power threshold for each divertor material at which periodic pulses of energy cause excessive target erosion and large vapor expansion. Large vapor expansion leads to plasma contamination and possible termination in a disruption, even in renewable surface materials such as lithium where erosion is not a problem. Excessive erosion from vaporization and macroscopic particles/droplets formation may affect subsequent plasma operations and lead to much shorter lifetime.

Acknowledgement

Work is supported by the US Department of Energy, Office of Fusion Energy Science, under Contract W-31-109-Eng-38.

References

[1] A. Hassanein, I. Konkashbaev, J. Nucl. Mater. 273 (1999) 326.

[2] A. Hassanein, Fusion Eng. Des. 56&57 (2001) 409.
[3] D.N. Hill, J. Nucl. Mater. 241–243 (1997) 182.
[4] R.J. Groebner, M.E. Fenstermacher, T.H. Osborne, et al., IAEA Technical Committee Meeting on Divertor Concepts, 11–14 September 2001, Aix-en-Provence, France.
[5] N. Ohyabu, T. Watanabe, H. Ji, H. Akao, et al., Nucl. Fusion 34 (1994) 387.
[6] A. Hassanein, I. Konkashbaev, J. Phys. Plasmas 63 (2000) 355.
[7] A. Hassanein, Fusion Eng. Des. 60 (2002) 527.